Te-Centric View of the Phase Change Mechanism in Ge-Sb-Te Alloys

S. Sen,[1] T. G. Edwards,[1] J.-Y. Cho,[2] and Y.-C. Joo[2]

[1]*Department of Chemical Engineering and Materials Science, University of California at Davis, Davis, California 95616, USA*
[2]*Department of Materials Science and Engineering, Seoul National University, Seoul, Korea*

(Received 20 December 2011; published 11 May 2012)

The short-range structure of amorphous and fcc $Ge_1Sb_2Te_4$ and $Ge_2Sb_2Te_5$ phase-change alloys is investigated using ^{125}Te NMR spectroscopy. Both amorphous and fcc structures consist solely of heteropolar Ge/Sb-Te bonds that may enable rapid displacive phase transformation without the need for extensive atomic rearrangement. The vacancy distribution is random in microcrystalline fcc phases while significant clustering is observed in their nanocrystalline counterparts that may result in the formation of tetrahedrally coordinated Ge atoms in the latter. This structural commonality may further facilitate the kinetics of transformation between amorphous and nanocrystalline fcc phases, a situation relevant for high-density memory storage.

DOI: 10.1103/PhysRevLett.108.195506 PACS numbers: 61.43.Dq, 64.70.kd, 76.60.Cq

Phase-change materials are of extraordinary technological importance in both optical and electronic rewritable data storage applications [1,2]. Alloys along the GeTe-Sb_2Te_3 tie line, in particular, $Ge_1Sb_2Te_4$ (GST124) and $Ge_2Sb_2Te_5$ (GST225), are materials of choice for such applications [1–4]. Large differences in optical reflectivity or electrical resistivity between the crystalline and amorphous phases of these materials provide a means to store binary information. For example, in the case of optical storage devices (e.g. CD, DVD, and Blu-Ray) the differences in optical reflectivity must be combined with a rapid and repeatable switching between the amorphous and the crystalline phases [5–8]. This phase switching, typically induced by local heating using a laser or a voltage pulse (Joule heating), occurs on nanosecond time scales indicating practically diffusionless transformation and therefore suggests structural similarities between the two phases [9]. On the other hand, the large change in optical reflectivity between the two phases is indicative of significant underlying differences in their electronic structures [5–8]. For GST124 and GST225 phases, switching occurs between the amorphous and a metastable fcc crystalline phase. However, the atomic scale mechanism of the phase-change process is not well understood, largely due to the fact that the structures of both the amorphous and the crystalline phases have remained highly controversial to date.

The fcc GST phase is characterized by a rocksalt structure with Te atoms completely occupying the *A* sites while Ge and Sb atoms are distributed over the *B* sites. The stoichiometry of the GST124 (GST225) phase requires 25% (20%) of the *B* sites to remain vacant. Therefore, the Ge and Sb atoms are octahedrally coordinated to Te while the average coordination number of Te would be 20% to 25% lower than the nominal value of six. The nature of the distribution of the vacancies on the *B* sites in the lattice remains unclear and cannot be uniquely determined using diffraction based techniques. The conventional model of the fcc crystal structure assumes a random distribution of vacancies over the Ge/Sb sublattice [4,10]. On the other hand, a recent study based on electron microscopy and diffraction has suggested significant vacancy clustering in the fcc phase [11].

Previous studies of the amorphous GST thin films based on x-ray diffraction and x-ray absorption spectroscopy have indicated that Ge, Sb, and Te atoms follow the 8-*n* coordination rule; i.e., these atoms are 4, 3, and 2 coordinated, respectively [12–14]. This structural model implies that the amorphous GST phases along the GeTe-Sb_2Te_3 join are Te deficient and hence, would contain ''wrong'' Ge/Sb-Ge/Sb bonds. A recent structural study based on extended x-ray-absorption fine structure spectroscopy has indeed suggested the formation Ge-Ge homopolar bonds in amorphous GST225 [14]. On the other hand, simulations of Ge *K*-edge XANES data have indicated significant structural differences between the melt-quenched and the as-deposited amorphous GST225 [15]. The melt-quenched phase was suggested to contain a mixture of Ge3:Te3, Ge4:Te2, and distorted octahedral Ge-Te configurations while the as-deposited amorphous phase is characterized by only the Ge4:Te2 configurations and a significant concentration of Ge/Sb-Ge/Sb bonds.

These competing structural models of the crystalline and amorphous GST phases imply different structural pathways and kinetics for the phase-change process. For example, the presence of a mixture of Ge3:Te3, Ge4:Te2, and distorted octahedral Ge-Te configurations and the absence of Ge-Ge and Ge-Sb bonds in the melt-quenched phase would imply a significant degree of short-range structural similarity between itself and the crystalline phase that would be consistent with fast phase-change kinetics. Kolobov and co-workers suggested an ''umbrella flip'' mechanism for the Ge atoms as the structural pathway for an ultrafast phase-change process [9]. According to this structural model of displacive transition, the Ge atoms

occupy distorted octahedral positions in the crystalline phase and the application of an intense laser pulse results in the rupture of weaker (i.e. longer) Ge-Te bonds and a ''flipping'' of the Ge into tetrahedral sites characteristic of the amorphous phase. A similar flipping process can also be envisaged for the Sb atoms from octahedral to pyramidal positions. However, if a significant fraction of the Ge atoms are already present in a tetrahedral environment in the fcc phase then the umbrella flip model may not play a significant role in the phase-change process [11]. In contrast, the presence of Ge/Sb-Ge/Sb bonds in the amorphous or melt-quenched phase would imply that such bonds need to be broken and rearranged during crystallization. Such a reconstructive structural transformation may not be consistent with the observed nanosecond time scale of the phase change.

Therefore, it is clear that the application of additional element-specific spectroscopic techniques is needed to resolve these controversies regarding the structures of the amorphous and crystalline GST phases in order to enable the development of a self-consistent structural model of the phase-change process. Information on structural changes around Te atoms in phase-change materials has been largely missing in the literature. This Te-centric view would be rather crucial since the presence of vacancies is expected to result in multiple coordination states for Te atoms in the fcc phase while in the amorphous phase one expects to have Te in twofold and/or threefold coordination with Ge/Sb atoms. It has been recently shown that ^{125}Te nuclear magnetic resonance (NMR) spectroscopy can be a particularly sensitive technique to study changes in the short-range order and coordination environment of Te atoms in tellurides [16,17]. The dominant contribution to the ^{125}Te NMR shift in semiconducting tellurides such as the GST materials is the chemical shift resulting from magnetic shielding caused by bonding electrons in covalent bonds [16]. The corresponding NMR shifts range typically between 1000 and -5000 ppm [16,17]. In contrast, the ^{125}Te NMR shifts in transition metal tellurides are located between $\sim$1000 and 8000 ppm and are dominated by the Knight shift resulting from the hyperfine coupling between the ^{125}Te nuclides and the delocalized electrons. Therefore, ^{125}Te NMR spectroscopy of tellurides is nontrivial to perform in the solid state where the incredibly large range of NMR shifts requires application of frequency-sweeping techniques to resolve the line shape. Nevertheless, a clear correlation has been found between the ^{125}Te NMR shifts and the tellurium nearest-neighbor coordination number, local site symmetry, and degree of covalency in bonding in Ge-Sb-As tellurides as well as in transition metal tellurides [16,17]. Here we present the results of a ^{125}Te NMR spectroscopic study of amorphous and crystallized GST phase-change materials to directly address the issue of vacancy distribution around the Te atoms in the fcc phase as well as the Te coordination environments in the amorphous phase. The results presented here provide, for the first time, a Te-centric view of the structures of GST phases.

Thin films of GST225 and GST124 with 300 nm thickness were deposited on 4 in diameter glass substrates using dc magnetron sputtering of the corresponding alloy targets. The deposition was conducted at room temperature with a background pressure below 10^{-3} Pa and a sputtering power of 80 W [18]. The as-deposited films were subsequently scraped off using a razor blade and 50 to 60 mg samples were recovered for ^{125}Te NMR spectroscopy. Powder x-ray diffraction measurements indicated that the GST225 as-deposited film consisted of a mixture of the amorphous phase and nanocrystalline fcc phase with an average crystallite size of $\sim$9 to 12 nm (see Supplemental Material [19]). On the other hand, the as-deposited GST124 film was found to be completely x-ray amorphous. Subsequent to the ^{125}Te NMR characterization, the powders obtained from these as-deposited amorphous films were isothermally heated at 200 °C for 7 minutes under vacuum to completely convert them into the fcc phase. An analysis of the x-ray diffraction powder pattern indicated significant strain related broadening of the Bragg peaks with average crystallite sizes of at least several tenths of a micron (see Supplemental Material [19]).

All ^{125}Te wideline NMR measurements were performed using a Bruker Avance 500 spectrometer operating at a ^{125}Te Larmor frequency of 158 MHz and a Bruker 4 mm magic-angle-spinning probe. The crystalline samples were mixed with insulating SiO_2 powder in order to enhance the penetration of the radio frequency field and to improve the probe tuning [16,17]. A single-pulse sequence with a $\pi/2$ pulse (3.0 μs) and a recycle delay of 1 s was used. As the ^{125}Te line shapes in these materials can span a frequency range of nearly 1 MHz, all NMR spectra reported here were acquired using a frequency-sweep technique outlined in detail in a previous publication [17]. The spectrometer frequency was swept from 157.0 to 158.0 MHz in increments of 0.1 MHz and approximately 7200 to 11 000 free induction decays were averaged to obtain the line shape at each frequency step. Line shapes collected at various frequencies were subsequently added to produce the final spectrum.

The ^{125}Te wideline NMR spectra of the GST225 and GST124 fcc phases are shown in Fig. 1. Both spectra display three clearly resolved broad signals centered around ~ -3800, -2800, and 200 to 600 ppm. On the basis of the previously established ^{125}Te NMR chemical shift scale for Ge-Sb-As tellurides, these three ^{125}Te NMR signals can be readily assigned to 6 (Te^{VI}), 4 + 5 (Te^{IV+V}), and 2 + 3 (Te^{II+III}) coordinated Te atoms, respectively, in these fcc crystal structures. It should be noted that a coordination number of N for a Te atom in the fcc phase implies the presence of 6-N Ge/Sb vacancies in its nearest neighbor coordination shell. The areas under NMR signals

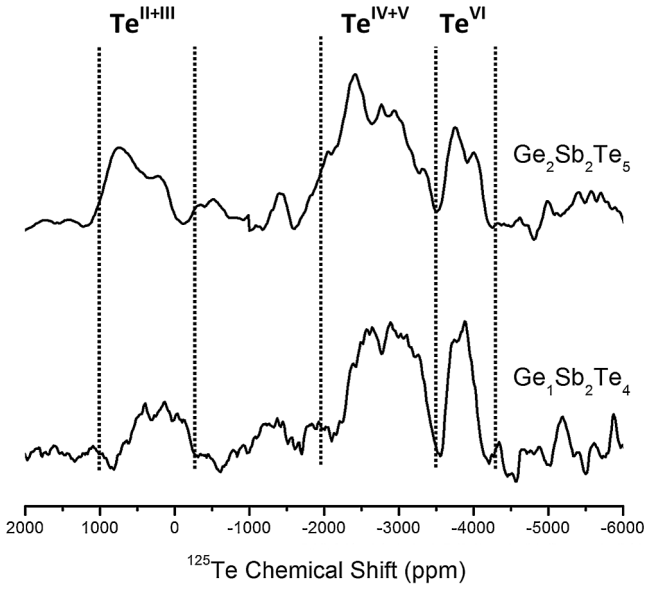

FIG. 1. ^{125}Te wideline NMR spectra of fcc-$Ge_2Sb_2Te_5$ (top) and fcc-$Ge_1Sb_2Te_4$ (bottom) phases. The ^{125}Te NMR chemical shift ranges for the peaks corresponding to Te^{II+III}, Te^{IV+V}, and Te^{VI} environments are as shown.

across a spectrum are simply proportional to the number of atoms in different chemical environments in a sample. Hence, the relative fractions of the various Te sites can be estimated from the respective areas under these ^{125}Te NMR signals. The Te^{VI}:Te^{IV+V}:Te^{II+III} ratios are found to be 25:66:9 for the GST225 crystal and 20:64:16 for the GST124 crystal. In the case of a random binomial distribution of vacancies in the nearest neighbor shell of Te, the probability of finding Te sites with n nearest neighbor vacancies in GST225 and GST124 fcc structures is given by ${}^6C_n{}^*(0.2)^n(0.8)^{6-n}$ and ${}^6C_n{}^*(0.25)^n(0.75)^{6-n}$, respectively. This expression yields the relative fractions for Te^{VI}, Te^{V}, Te^{IV}, Te^{III}, and Te^{II} environments (i.e., Te with 0, 1 ,2 , 3, and 4 vacancies) in GST225 (GST124) to be 26.2% (17.9%), 39.3% (35.7%), 24.6% (29.8%), 8.2% (13.3%), and 1.5% (3.3%), respectively. These population fractions are remarkably consistent with the above mentioned Te^{VI}:Te^{IV+V}:Te^{II+III} ratios estimated from the ^{125}Te NMR spectra of the two fcc GST phases and indicate a random distribution of vacancies around Te atoms in the fcc structures. These results also refute the possibility of the presence of nearly 35% of the Ge atoms in fourfold coordination in these crystal structures (as has been suggested in a recent study [11]) since that would require a strong clustering of vacancies and hence a significant departure from random distribution. For example, 35% tetrahedral Ge in fcc-GST225 would require, depending on the degree of clustering of such Ge environments, anywhere between ~20% and 56% of Te in the Te^{III} environment. This Te^{III} concentration in fcc GST225 is significantly higher than what is observed in this study and is expected from a random vacancy distribution (~ 8%).

The ^{125}Te wideline NMR spectrum of the amorphous GST124 phase is shown in Fig. 2. This spectrum displays two clearly resolved signals centered around ~500 and −400 ppm that can be readily assigned to Te^{II} and Te^{III} environments, respectively. Simulation of this ^{125}Te wideline NMR line shape indicates that the relative fractions of these two Te environments are nearly equal in amorphous GST124 and consequently the average coordination number of Te atoms in this material is approximately 2.5. Previous experimental studies based on Ge and Sb K-edge extended x-ray-absorption fine structure spectroscopy, x-ray and neutron diffraction, and ^{121}Sb NMR spectroscopy have indicated that in the amorphous GST phases the constituent Ge and Sb atoms are predominantly 4 and 3 coordinated, respectively [13,14,20]. It is intriguing to note that the average coordination numbers of 4, 3, and 2.5 for Ge, Sb, and Te atoms, respectively, are consistent with complete heteropolar bonding (i.e., only Ge-Te and Sb-Te bonds) in the amorphous GST124 phase since its chemical composition $GeSb_2Te_4$ can be expressed as $(GeTe_{4/2.5}) + 2^*(SbTe_{3/2.5})$. This unique result is important in the mechanistic understanding of the phase-change process. This is because the presence of solely heteropolar bonding in both the amorphous and fcc phases can allow for rapid displacive motion of the constituent atoms to be sufficient to transform the structure of one phase into another, a scenario that is consistent with the ultrafast kinetics characteristic of the phase-change process [9]. On the other hand, for an average Te coordination number less than 2.5 the structure of the amorphous phase would have to contain Ge/Sb -Ge/Sb bonds in order to satisfy the coordination number requirements for Ge and Sb. Therefore, it would require extensive bond breaking and rearrangement along with atomic diffusion beyond the

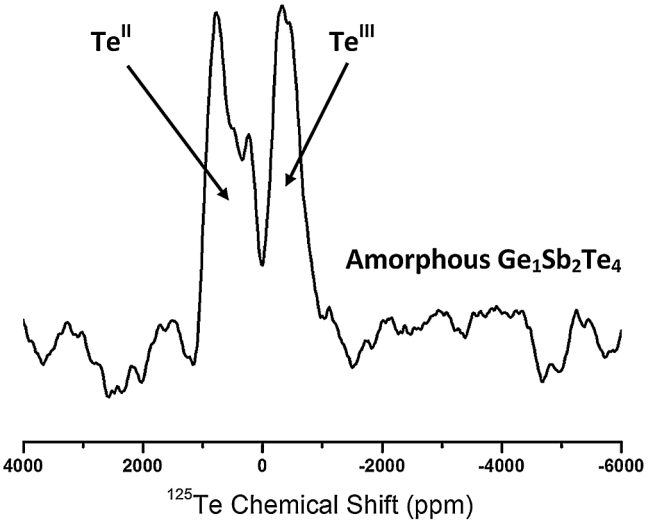

FIG. 2. ^{125}Te wideline NMR spectrum of the amorphous $Ge_1Sb_2Te_4$ phase. Arrows indicate ^{125}Te resonances corresponding to the Te^{II} and Te^{III} environments.

nearest neighbor length scale for the transformation of amorphous GST124 into the heteropolar bonded fcc phase. Thus, such a process can be significantly slower than the displacive mechanism discussed above. The Te-centric view of the displacive phase-change mechanism is elucidated in Fig. 3, where the Ge and Sb atoms are displaced from octahedral to tetrahedral and pyramidal sites, respectively, and as a consequence the Te^{V} atom in the original fcc phase [Fig. 3(a)] transforms into a Te^{III} or a Te^{II} configuration characteristic of the amorphous phase [Fig. 3(b) and 3(c)].

A recent computational study has indicated that the large optical contrast between the fcc and amorphous GST phases can be explained by a destruction in the amorphous phase of the crystalline long-range alignment of the rows of resonantly bonded p orbitals via strong distortion without any change in the original octahedral coordination of the constituent atoms [21]. However, the present ^{125}Te NMR results indicate that the average coordination number of Te in the amorphous GST phase (~ 2.5) is quite close to its 8-n value of 2 and the corresponding NMR spectrum is rather distinct from what would be expected from a distorted fcc structure.

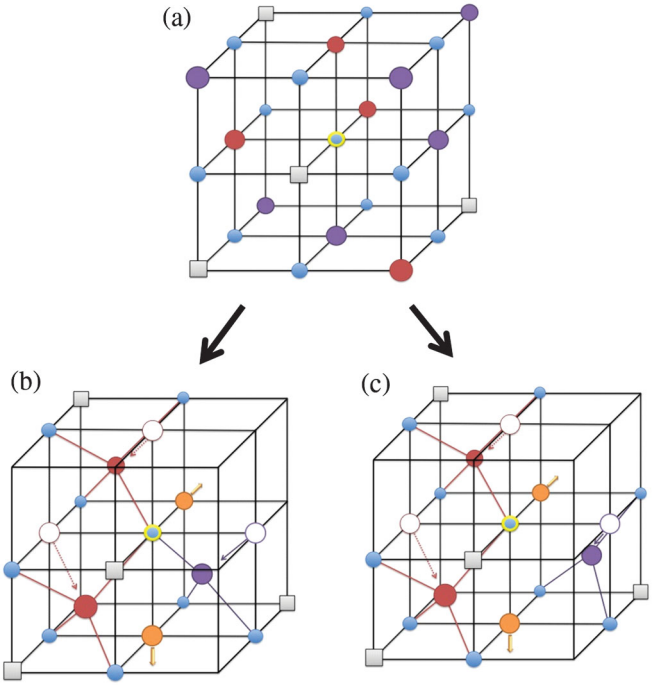

FIG. 3 (color). Ball-and-stick model of a Te-centric view of the phase-change process involving the transformation of (a) an original Te^{V} environment the fcc phase (shown as a blue sphere with an yellow shell at the center of the cells) into (b) a Te^{III} environment or (c) a Te^{II} environment that are characteristic of the amorphous phase. The transformation is mediated via the displacive motion of the neighboring Ge and Sb atoms (akin to the umbrella flip motion proposed in [9]) into tetrahedral and pyramidal positions, respectively. The Te, Ge, and Sb atoms are shown as blue, brown, and purple spheres, respectively. Original vacancies in the fcc structure are shown as open squares. Open circles in (b) and (c) represent the original octahedral positions of Ge/Sb atoms in (a) that are displaced to tetrahedral and pyramidal positions within the cell. The initial and final positions are connected with arrows. Orange spheres in (b) and (c) represent Ge/Sb atoms that were originally in the cell in (a) but get displaced out of the cell in (b) and (c).

As mentioned earlier, the as-deposited GST225 films consist of a mixture of the amorphous phase and nanocrystalline fcc phase. The ^{125}Te wideline NMR spectrum of this material is shown in Fig. 4. This spectrum shows that Te atoms are mostly in Te^{II} + Te^{III} and Te^{IV} + Te^{V} configurations and, according to the discussion above, the former sites are mostly in the structure of the residual amorphous phase while the latter must belong exclusively to the fcc phase. Besides these Te sites, the spectrum also contains a resonance corresponding to a small fraction of Te^{VI} sites in the fcc phase (Fig. 4). The Te^{VI}:Te^{IV+V} ratio in the nanocrystalline fcc phase is 1:6, which is significantly smaller than 1:2.6 in the microcrystalline phase as seen in Fig. 1. Therefore, compared to the microcrystalline fcc phase, the nanocrystalline fcc phase is characterized by a smaller fraction of Te^{VI} sites, indicating significant vacancy clustering in the latter. Such vacancy clustering may result in strong Ge-vacancy interactions and the formation of domains of Ge atoms in the tetrahedral environment in the fcc phase [11]. Consequently, the similarity between the amorphous and nanocrystalline fcc phases in their Ge coordination environments may contribute to the rapid reversibility of the amorphous ↔ fcc phase-change process in a real device. This can become particularly important in the case of high-density memory storage applications where the feature or bit size needs to be kept at the nanometer scale [22].

In summary, the ^{125}Te NMR results presented here bridge an important gap in our current understanding of

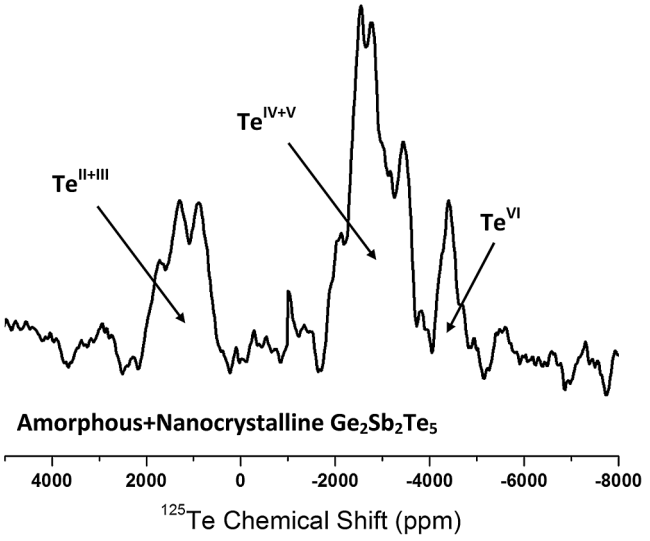

FIG. 4. ^{125}Te wideline NMR spectrum of the mixed amorphous^{+} nanocrystalline fcc $Ge_2Sb_2Te_5$ phase. Arrows indicate ^{125}Te resonances corresponding to Te^{II+III}, Te^{IV+V}, and Te^{VI} environments.

the structural characteristics of phase-change materials. The microcrystalline fcc GST phases are characterized by a random distribution of vacancies in the Ge/Sb sites while significant vacancy clustering is observed in their nanocrystalline counterparts. On the other hand, the amorphous GST phases are characterized by mixed Te coordination environments that preclude the presence of any Ge/Sb-Ge/Sb homopolar bonding. The resulting short-range structural commonalities between the microcrystalline fcc and amorphous phases in the form of exclusive heteropolar Ge/Sb-Te bonding and the possible presence of a substantial fraction of Ge in a tetrahedral environment in the nanocrystalline fcc phase are consistent with a phase-change mechanism dominated by short-range displacements of the constituent atoms.

This work was supported by NSF Grant No. DMR-1104869.

[1] E. R. Meinders, A. V. Mijritskii, L. van Pieterson, and M. Wuttig, *Optical Data Storage: Phase Change Media and Recording* (Springer, Berlin, 2006).
[2] S. Raoux, W. Welnic, and D. Lelmini, Chem. Rev. **110**, 240 (2010).
[3] M. Wuttig, Nature Mater. **4**, 265 (2005).
[4] M. Wuttig and N. Yamada, Nature Mater. **6**, 824 (2007).
[5] W. Welnic, A. Pamungkas, R. Detemple, C. Steimer, S. Blügel, and M. Wuttig, Nature Mater. **5**, 56 (2006).
[6] W. Welnic, S. Botti, L. Reining, and M. Wuttig, Phys. Rev. Lett. **98**, 236403 (2007).
[7] M. Wuttig, D. Lüsebrink, D. Wamwangi, W. Wenic, M. Gilleen, and R. Dronskowski, Nature Mater. **6**, 122 (2007).
[8] K. Shportko, S. Kremers, M. Woda, D. Lencer, J. Robertson, and M. Wuttig, Nature Mater. **7**, 653 (2008).
[9] A. V. Kolobov, P. Fons, A. I. Frenkel, A. L. Ankudinov, J. Tominaga, and T. Uruga, Nature Mater. **3**, 703 (2004).
[10] N. Yamada and T. Matsunaga, J. Appl. Phys. **88**, 7020 (2000).
[11] X. Q. Liu, X. B. Li, L. Zhang, Y. Q. Cheng, Z. G. Yan, M. Xu, X. D. Han, S. B. Zhang, Z. Zhang, and E. Ma, Phys. Rev. Lett. **106**, 025501 (2011).
[12] S. Kohara *et al.*, Appl. Phys. Lett. **89**, 201910 (2006).
[13] P. Jovari, I. Kaban, J. Steiner, B. Beuneu, A. Schops, and M. A. Webb, Phys. Rev. B **77**, 035202 (2008).
[14] D. A. Baker, M. A. Paesler, G. Lucovsky, S. C. Agarwal, and P. C. Taylor, Phys. Rev. Lett. **96**, 255501 (2006).
[15] M. Krbal, A. V. Kolobov, P. Fons, J. Tominaga, S. R. Elliott, J. Hegedus, and T. Uruga, Phys. Rev. B **83**, 054203 (2011).
[16] I. Orion, J. Rocha, S. Jobic, V. Abadie, R. Brec, C. Fernandez, and J. P. Amoureux, J. Chem. Soc. Dalton Trans. **1997**, 3741 (1997).
[17] T. G. Edwards, E. L. Gjersing, S. Sen, S. C. Currie, and B. G. Aitken, J. Non-Cryst. Solids **357**, 3036 (2011).
[18] I.-M. Park, J.-K. Jung, S.-O. Ryu, K.-J. Choi, B.-G. Yu, Y.-B. Park, S. M. Han, and Y.-C. Joo, Thin Solid Films **517**, 848 (2008).
[19] See Supplemental Material at http://link.aps.org/supplemental/10.1103/PhysRevLett.108.195506 for details on the methodology used to determine crystallite size from x-ray powder diffraction data.
[20] D. C. Bobela, P. C. Taylor, P. Kuhns, A. Reyes, and A. Edwards, Phys. Rev. B **83**, 033201 (2011).
[21] B. Huang and J. Robertson, Phys. Rev. B **81**, 081204(R) (2010).
[22] H. F. Hamann, M. O'Boyle, Y. C. Martin, M. Rooks, and H. K. Wickramasinghe, Nature Mater. **5**, 383 (2006).